Ultrasensitive Impedimetric Lectin Biosensors with Efficient Antifouling Properties Applied in Glycoprofiling of Human Serum Samples

Tomas Bertok[a], Ludmila Klukova[a], Alena Sediva[a], Peter Kasak[b], Vladislav Semak[b], Matej Micusik[b], Maria Omastovab, Lucia Chovanova[c], Miroslav Vlcek[c], Richard Imrich[c], Alica Vikartovska[a], Jan Tkac[a*]

[a] *Department of Glycobiotechnology, Institute of Chemistry, Slovak Academy of Sciences, Dúbravská cesta 9, 845 38, Bratislava, Slovak Republic;*

[b] *Center for Advanced Materials, Qatar University, P.O.Box 2713 Doha, Qatar;*

[c] *Laboratory of Human Endocrinology,Institute of Experimental Endocrinology, Slovak Academy of Sciences, Vlárska 3, 833 06, Bratislava, Slovak Republic*

[*] Corresponding author: Jan.Tkac@savba.sk, Tel.: +421 2 5941 0263, Fax: +421 2 5941 0222

- **Abstract**

Ultrasensitive impedimetric lectin biosensors recognizing different glycan entities on serum glycoproteins were constructed. Lectins were immobilized on a novel mixed self-assembled monolayer containing 11-mercaptoundecanoic acid for covalent immobilization of lectins and betaine terminated thiol to resist nonspecific interactions. Construction of biosensors based on Concanavalin A (Con A), Sambucus nigra agglutinin type I (SNA), and Ricinus communis agglutinin (RCA) on polycrystalline gold electrodes was optimized and characterized with a battery of tools including electrochemical impedance spectroscopy, various electrochemical techniques, quartz crystal microbalance (QCM), Fourier transform infrared (FT-IR) spectroscopy, atomic force microscopy (AFM), and X-ray photoelectron spectroscopy (XPS) and compared with a protein/lectin microarray. The lectin biosensors were able to detect glycoproteins from 1 fM (Con A), 10 fM (Ricinus communis agglutinin (RCA), or 100 fM (SNA) with a linear range spanning 6 (SNA), 7 (RCA), or 8 (Con A) orders of magnitude. Furthermore, a detection limit for the Con A biosensor down to 1 aM was achieved in a sandwich configuration. A nonspecific binding of proteins for the Con A biosensor was only 6.1% (probed with an oxidized invertase) of the signal toward its analyte invertase and a negligible nonspecific interaction of the Con A biosensor was observed in diluted human sera (1000×), as well. The performance of the lectin biosensors was finally tested by glycoprofiling of human serum samples from healthy individuals and those having rheumatoid arthritis, which resulted in a distinct glycan pattern between these two groups.

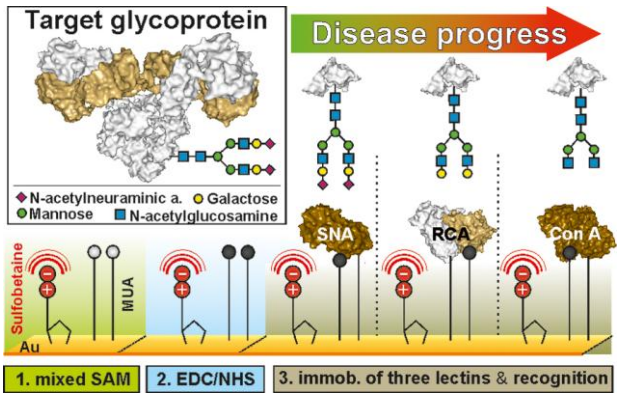

Since the introduction of DNA microarrays in 1995,[1] the technology has been heavily applied in analysis of genomewide expression in order to get information about possible functions of novel or poorly characterized genes[2] and for diagnostic purposes, as well.[3] Even though DNA microarray technology has shed light on many physiological states by analysis of expression of gene clusters, there is usually very low correlation between RNA and protein abundance detected in single-cell organisms[4] as well as in higher ones, including humans.[5] Since quantitative analysis of proteins is central to proteomics with a focus on design of novel drugs, diagnosis of diseases, and their therapeutic applications, protein microarrays were successfully launched to address these issues.[6] Analysis of finely tuned post-translational modifications (PTMs) of proteins,[7] considering addition of a small functionality such as single phosphorylation can change activity of a protein up to 108 times,[8] is an additional challenge for current analytical technology. Glycosylation is another and highly abundant form of PTM of proteins, and it is estimated that 70% of proteins in humans together with 80% of membrane-bound proteins are glycosylated.[9] Glycan mediated recognition plays an important role in cell physiology(fertilization, immune response, differentiation of cells, cell−matrix interaction, cell−cell adhesion, etc.).[10] Glycans, as highly abundant ligands on the surface of cells, are naturally involved in pathological processes triggered by adhesion of viruses, bacteria, and parasites to host cells, in neurological disorder and in tumor growth and metastasis.[3,11] Thus, better understanding of glycan mediated pathogenesis can establish a "policy" to develop more efficient strategies for disease treatment with few recent studies as good examples, e.g., "neutralization" of various forms of viruses[12] or more efficient vaccines against various diseases.[13] Changes of protein glycosylation can be effectively applied in early stage diagnostics of several diseases, including different forms of cancer with known

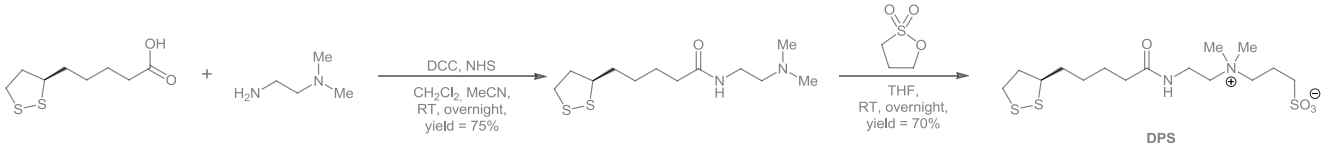

Scheme 1.: Synthesis of DPS.

glycan-based biomarkers.[14] Moreover, many previously established and even commercially successful strategies used to treat diseases are currently being revisited in light of glycan recognition in order to lower side effects, enhance serum half-life, or decrease cellular toxicity.[3,15] Recently, the first glyco-engineered antibody was approved to the market, what was called by the authors "a triumph for glyco-engineering".[16] Glycomics focuses on revealing finely tuned reading mechanisms in the cell orchestra based on graded affinity, avidity, and multivalency of glycans (i.e., sugar chains covalently attached to proteins and lipids).[17] Glycans are ideal information coding tools since they can form enormous numbers of possible unique sequences from basic building units. The theoretical number of all possible hexamers for glycans is 8 orders of magnitude larger than the theoretical number of peptides and 11 orders of magnitude larger than the theoretical number of DNA sequences.[18] It is estimated that the size of the cellular glycome can be up to 500 000 glycan modified biomolecules (proteins and lipids) formed from 7000 unique glycan sequences.[19] This variation can explain human complexity in light of a paradoxically small genome. This glycan complexity together with similar physicochemical properties of glycans is the main reason why progress in the field of glycomics has been behind advances in genomics and proteomics.[20] Traditional glycoprofiling protocols rely on glycan release from a biomolecule with subsequent quantification by an array of techniques including capillary electrophoresis, liquid chromatography, and mass spectrometry.[21] There is an alternative way for glycoprofiling by application of lectins (natural glycan recognizing proteins[18,22]) in combination with various transducing protocols.[11b,23] The most powerful glycoprofiling tool relies on lectins arrayed on solid surfaces for direct analysis of glycoproteins, glycolipids, membranes, and even glycans on the surface of intact cells.[24] Even though lectin microarrays offer high throughput assay protocols with a minute consumption of samples and reagents, there are some drawbacks such as the need to fluorescently label the sample or the lectin, which negatively affects the performance of detection,[11a,b] relatively high detection limits, and quite narrow working concentration ranges. The use of nanotechnology, sophisticated patterning protocols, and advanced detection platforms can help overcome the drawbacks of lectin microarray technology allowing it to work in a label-free mode of operation, with high sensitivity, low detection limits, and a wide concentration window, and in some cases, real time analysis of a binding event is possible.[10b,25] In our recent work, we focused on development of ultrasensitive impedimetric lectin biosensors with detection limits down to the single-molecule level based on controlled architecture at the nanoscale,[25e,26] but such biosensors were prone to nonspecific interactions. The main aim of this manuscript was to develop a patterning protocol based on a mixed self-assembled monolayer (SAM) layer containing one derivative available for covalent immobilization of lectins and a sulfobetaine derivative ((R)-3-((2-(5-(1,2-dithiolan-3-yl)-pentanamido)ethyl)dimethylammonio)propane-1-sulfonate (DPS) Scheme 1) forming an interfacial layer (Figure S1, Supporting Information) effectively blocking nonspecific interactions.[27] This strategy allowed us to detect changes in a glycoprofile in complex human samples with a detection limit down to the fM level. The biosensors, based on three different lectins, were calibrated using 4 different glycoproteins (Figure S2, Supporting Information), and finally, its reliability was proved in complex samples, suggesting this concept can be integrated into an array format of analysis.

- **Experimental Section**

Chemicals

11-Mercaptoundecanoic acid (MUA), potassium hexacyanoferrate(III), potassium hexacyanoferrate(II) trihydrate, sodium chroride, potassium chloride, 1,3-propane sultone, N-hydroxysuccinimide (NHS), N-(3-dimethylaminopropyl)-N′-ethylcarbodiimide hydrochloride (EDC), sodium sulfate, N,N-dimethylethylene diamine, dicyclohexylcarbodiimide (DCC), sodium periodate, ethylene glycol, ethanolamine, acetonitrile, dichloromethane, tetrahydrofuran (THF), glycine, hydrochloric acid, Tween 20, fetuin (FET, 8.7% of Nacetylneuraminic acid), asialofetuin (ASF, ≤ 0.5% of Nacetylneuraminic acid), invertase from Baker's yeasts (invertase, INV), transferrin (TRF), Ricinus communis agglutinin (Caution: handle with special care since it is a toxin), and concanavalin A were purchased from Sigma Aldrich (USA). (R)-Lipoic acid was purchased from TCI Europe. Sambucus nigra agglutinin type I (SNA) lectin from Sambucus nigra was purchased from Gentaur (Belgium). Ethanol for UV/vis spectroscopy (ultra pure) was purchased from Slavus (Slovakia). Zeba spin desalting columns (40k MWCO) for protein purification were purchased from Thermo Scientific (UK). All buffer components were dissolved in deionized water (DW).

Preparation of a Biorecognition Surface

On an electrode modified by a mixed SAM, as described in the Supporting Information, the biorecognition elements (different lectins) were immobilized using standard amine coupling with the carboxylic

groups of MUA activated by a 1 to 1 mixture of 0.2 M EDC and 0.05 M NHS. The incubation of the electrode in a mixture of EDC/NHS took 15 min, and the surface was washed by DW. Lectins were covalently immobilized on the activated SAM layer in a 10 μM stock solution (40 μL) in a 100.05% Tween 20 by incubation for 1 h in the dark and at room temperature. After the immobilization was completed, the surface was gently rinsed by DW and incubated with 10 mM M HCl for 3 min, rinsed by DW, incubated with 10 mM glycine−HCl (pH 2.5) for 3 min, and finally again rinsed by DW. This procedure was introduced for removal of noncovalently bound lectin molecules from the electrode.28 Incubation of the biosensor with the analyte was performed by incubation with a stock solution of a glycoprotein or a sample (40 μL) for 20 min.

Assay Procedure

All electrochemical impedance spectroscopy (EIS) measurements were performed in an electrolyte containing 5 mM potassium hexacyanoferrate(III), 5 mM potassium hexacyanoferrate(II), and 0.1 M KCl. The analysis was run at 50 different frequencies (ranging from 0.1 Hz up to 100 kHz) under Nova Software 1.9 (Ecochemie, Netherlands). The acquired data were evaluated by the same software using a Nyquist plot with an equivalent circuit R(C[RW]) employed. The charge transfer resistance (RCT) parameter was used as the measure for the calibration of the biosensor and for real sample measurements. Each analyte/sample was measured at least in triplicate with an independent biosensor device, and results are shown with a standard deviation (±SD) calculated in Excel. Human serum samples were diluted in 10 mM PBS buffer, pH 7.4. All stock solutions (lectins, standard glycoproteins, and human sera) were stored at −20 °C in aliquots.

- **Results and Discussion**

Characterization of SAM Modified Gold Surface

In order to get information about the surface coverage of DPS within single and mixed SAM layers on a planar gold surface, characterization by X-ray photoelectron spectroscopy (XPS) and an electrochemical reduction of the SAM were applied. XPS data were fitted in a way to fit the S2p spectrum with two doublets with S2p3 peaks centered at 161.9 and 163.5 eV, respectively, according to a previous study.[29] XPS showed a clear difference in the presence of various functionalities. When pure SAM layers of MUA and DPS were compared (Figure 1), peaks attributed to SO_3^{2-} and S−S groups were observed only in the spectra of DPS (Figure 1A). More detailed analysis of a mixed SAM composed of MUA and DPS by XPS revealed increased amounts of DPS (signal from SO_3^{2-} group was plotted) as the amount of DPS in a mixture with MUA was decreasing with the highest surface amount reached at a ratio of DPS/MUA of 1 to 1 (Figure S3, Supporting Information). The results from reductive desorption of thiols can be used to get quantitative information about the surface coverage of thiols.[30] A pure DPS SAM layer revealed a surface density of 1.97 molecules nm^{-2}, a value that is in excellent agreement with values from 1.8 to 2.1 molecules nm−2 obtained previously for thioctic acid.[31] Moreover, quantification of DPS in mixed SAM layers by reductive desorption was possible since the onset potential of reductive desorption of DPS and MUA was different. Analysis of a mixed SAM sample by reductive desorption provided a value of 2.66 molecules nm^{-2} of DPS in a SAM prepared from a 1 to 1 mixture of MUA and DPS (Figure S3, Supporting Information). Higher surface coverage of DPS within a mixed SAM compared to a pure SAM can be explained by a lower repulsion between SO_3^- groups of neighboring DPS molecules present in the mixed SAM. Recently, it was observed that the density of a mixed SAM composed of 2-aminoethanethiol and 2-mercaptoethanesulfonic acid is higher compared to corresponding pure monolayers, what was ascribed to the strong molecular interactions between these two components.[32] There are other reports describing a strong interaction between a SO_3^{2-} terminated thiol and a diluted one terminated in an −NH2 or −OH functional group influencing contact angle or zeta potential of mixed SAMs with changes in the monolayer composition.[33]

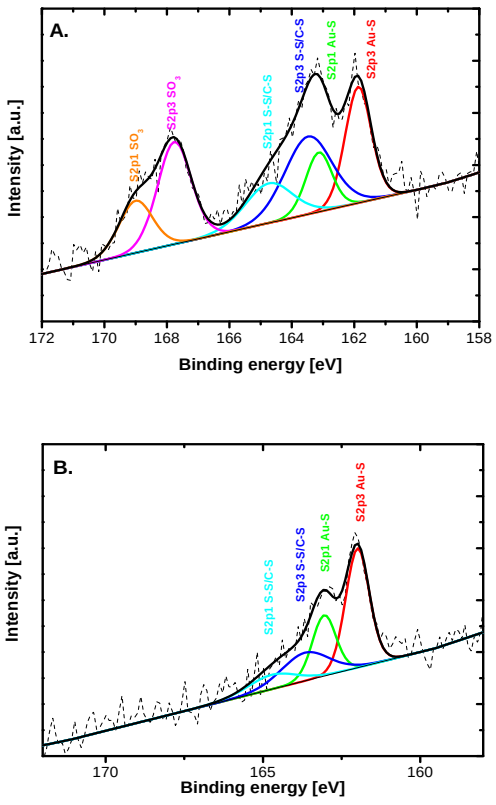

Fig. 1.: XPS of two different SAM layers showing present functional groups. A) pure SAM from a sulfobetaine derivative and B) pure SAM from MUA.

Quartz Crystal Microbalance (QCM) Experiments

A surface coverage of 11.3 pmol cm^{-2} for concanavalin A (Con lectin immobilized on the surface prepared from a 1 to 1 mixture of MUA and DPS was obtained from a QCM experiment (Figure S4, Supporting Information). Con A is composed of four identical subunits (Figure S5, Supporting Information). When a hard sphere model[34] was applied for calculation of a theoretical surface coverage of a Con A tetramer, a value of 4.8 pmol cm^{-2} was calculated. This calculated result does not correspond to the value obtained from a QCM experiment. Since Con A can dissociate into subunits under certain physicochemical conditions,[35] we tried to calculate what would be a theoretical surface coverage for a monomer of Con A, revealing a value of 12.1 pmol cm^{-2}, applying the same hard sphere model. These calculations suggest Con A dissociates into subunits after incubation with aheavily negatively charged surface occupying almost a full monolayer. Since INV has 18 glycosylation sites with glycans terminated in mannose units,[23]a we ran QCM measurements to see if it is possible to form a sandwich configuration. In this experiment, the Con A biosensor was incubated with INV and then Con A was injected over the biorecognition layer to complete a sandwich configuration (Figure S6, Supporting Information). The QCM experiment showed that INV was bound to the Con A biosensor with a surface density of 0.67 pmol cm^{-2} (Figure S7, Supporting Information), revealing a molar ratio INV/Con A of 0.055. This is in a good agreement with values of molar ratio from 0.02 to 0.17 obtained on various peptide aptamer surfaces.[36] The second Con A layer on a layer of INV wasformed with a surface density of 2.75 pmol cm^{-2} (Figure S7, Supporting Information), suggesting that every INV molecule on average interacted with 4 molecules of Con A present in the outer layer. There are two possible outputs of this observation. The first one is the observed decrease in the detection limit of the Con A biosensor, which is further explored in the section Con A Biosensor. The second more important application would be the formation of a sandwich configuration with a possibility to vary lectins involved in the formation of a second lectin layer. Such an approach can provide additional information about possible changes in the glycan profile at different glycosylation sites, which can be a useful tool in more detailed glycoprofiling of various proteins applicable in diagnostics.

Atomic Force Microscopy (AFM) Experiments

AFM images showed the surface is densely populated by Con A molecules (Figure 2). A detailed analysis of Con A spotsrevealed the presence of different forms of Con A with the heights of h = (3.6 ± 0.4) nm with a full width at half-maximum fwhm = (18 ± 1) nm, h = (5.4 ± 0.7) nm with fwhm = (26 ± 4), and h = (7.6 ± 0.4) nm with fwhm = (26 ± 4). These results suggest, besides the presence of monomers of Con A, most likely other forms of Con A such as dimers and tetramers (intact Con A molecules), might be present, as well. Indication that the spot of Con A with h = 7.6 nm is an intact Con A tetramer is supported by the thickness of Con A layer of 7.7 nm previously published.[37] For example, a Con A monomer[38] has the size 42 × 40 × 39 Å, a dimer of Con A39 has the size of 61 × 86 × 91 Å, and a tetramer[39] of Con A has the size of 67 × 113 × 122 Å. The lateral size of all Con A spots in AFM images is larger due to the tip convolution effect.[40] Moreover, a high density of Con A monomers on the surface is in good agreement with a similar conclusion made from the QCM results about preferential adsorption of Con A on the surface in a monomer form. This is supported by calculations made from a hard sphere model, when high fraction dimers and tetramers of Con A on the surface cannot make the surface coverage as read from the QCM experiment. A detailed analysis of AFM images revealed an increase of the roughness factor Rq from 0.8 nm for bare gold to 1.0 nm for gold modified by the SAM prepared from a 1 to 1 mixture of MUA and DPS (Figure S8, Supporting Information). Moreover, the surface roughness increased significantly to a value of 1.8 nm after immobilization of Con A lectin (Figure 2).

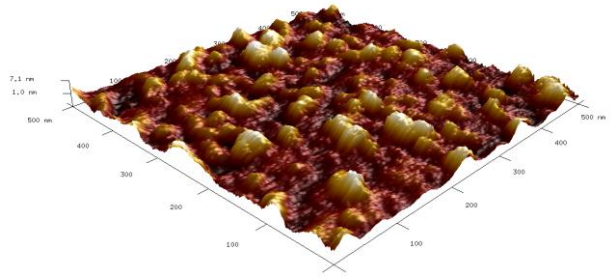

Fig. 2.: AFM image of the surface after immobilisation of Con A.

Con A Biosensor

The oxidized form of INV (oxINV) was prepared using sodium periodate in order to “destroy” glycan determinants on a protein backbone. This oxidized protein was used as a negative control during characterizations of the Con A biosensor. The Fourier transform infrared spectroscopy (FTIR) spectra of oxINV showed a decrease in the peaks corresponding to −OH groups (3250−3350 nm) and a small peak appeared at 1738 nm, attributed to the presence of free aldehyde groups (data not shown) after oxidation. The performance of the Con A biosensor was tested on five different surfaces prepared from a mixture of MUA/DPS having different molar ratios in a liquid phase (1:0, 3:1, 1:1, 1:3, and0:1). When the Con A biosensor was built on a pure MUA layer (1:0), incubation with INV and oxINV did not provide a well resolved semicircle in a Nyquist plot and thus RCT could not be obtained, as already shown.[26a] The Con A biosensor prepared on a SAM from a 3:1 mixture did not discriminate between INV and oxINV, suggesting that the response is only due to nonspecific interaction, e.g., electrostatic interactions with predominant −COOH groups (Figure S9A, Supporting Information). The Con A biosensor prepared on the SAM froma 1:1 and 1:3 mixture showed the ability of the Con A

biosensor to selectively detect INV (Figure 3 and Figure S9B, Supporting Information), but the Con A biosensor built-up on a surface deposited from a 1:1 MUA/DPS mixture provided better performance (Figure 3). The Con A biosensor preparedon a pure DPS SAM layer was completely resistant to any protein binding (Figure S9C, Supporting Information). Thus, for further experiments, the Con A biosensor prepared on a mixed SAM layer from a 1:1 mixture MUA/DPS was used, showing excellent selectivity for INV in comparison to oxINV detection (Figure S10, Supporting Information).

Besides strong interaction, Con A exhibits with oligomannose glycans (Scheme 1) such as on INV (KD in the range of 0.1−0.4 μM);[23a] Con A also interacts weakly with complex glycans containing few mannose units and terminated in galactose or N-acetylneuraminic acid (Scheme 1) such as on TRF (KD in the range of 1−3 μM).[23a] Thus, the Con A biosensor was calibrated with 3 different glycoproteins INV, oxINV, and TRF, showing only 6.1% of the sensitivity for oxINV in comparison to INV (Figure 3). Moreover, the Con A biosensor showed 68% of the sensitivity for TRF in comparison to INV and a detection limit for TRF that was significantly shifted to higher values (≈1 pM), when compared to the detection limit for INV (≈1 fM). Linear range for the Con A biosensor toward INV was calculated from a concentration at which the signal for INV was above the signal for oxINV, considered to be blank. Quite a wide linear range spanning 4 orders of magnitude for biosensors based on EIS was observed,[41] but our lectin biosensor offering a linear response over 8 orders of magnitude has a feature essential for analysis of glycoproteins in complex samples where the amount of glycoproteins can vary over a large concentration window. As already indicated from the QCM measurements, formation of a sandwich configuration has the potential to further decrease the detection limit of the Con A biosensor down to ≈1 aM, that is clearly shown in Figure 3. The detection limit of our biosensor is much lower than for any lectin biosensor prepared to date,[10b,35] except for our recent lectin biosensor based on a 3-D nanointerface.[26b] The best detection limit for the lectin biosensors prepared by other groups was 20 fM[41b] or 150 fM.[41a] Moreover, the biosensor offers a linear response in the concentration window of at least 5 orders of magnitude.

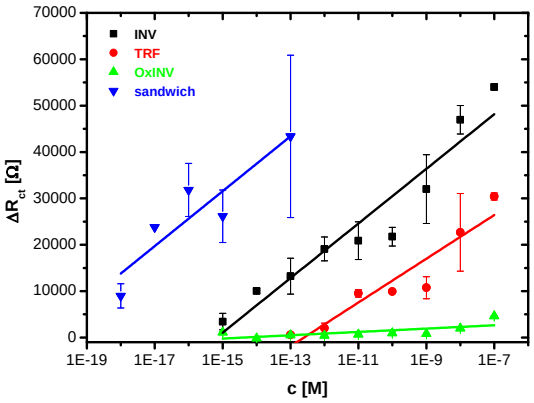

Fig. 3.: Calibration of the Con A impedimetric biosensor with various glycoproteins such as invertase (INV), transferrin (TRF) and oxidised invertase (oxINV) applied as a control. Moreover, a calibration for the sandwich biosensor configuration with additional outer lectin layer applied (see Fig. S6) is shown, as well. Each analyte was measured at least in triplicate with an independent biosensor device and results are shown with a standard deviation (± SD) calculated in Excel.

SNA and Ricinus communis Agglutinin (RCA) Lectin Biosensors

The composition of an interfacial SAM layer being optimal for the Con A biosensor (1:1 MUA/DPS) was chosen for construction of the SNA and RCA biosensors, since all lectins have approximately the same size (112−140 kDa). Linear range for the SNA and RCA biosensors were calculated from the concentration at which the signal for the analyte was above the background signal, shown as a thin line (Figures 4 and 5). The SNA biosensor recognizing N-acetylneuraminic acid was calibrated with two analytes FET (8.7% of N-acetylneuraminic acid) and ASF (≤0.5% of N-acetylneuraminic acid). The SNA biosensor started to interact with FET at a concentration of 100 fM, while ASF was recognized by the SNA biosensor at a concentration of 1 pM (Figure 4). The sensitivity ratio of the SNA biosensor for these two analytes derived from the linear part of their concentration dependence, of 4.8, is in agreement with a previously obtained value of 7.6.[26b] The RCA biosensor detecting terminal galactose on glycans was calibrated with FET and ASF, as well. ASF, which is a better analyte for the RCA biosensor compared to FET, was detected at a concentration of 10 fM with a much higher sensitivity (13×) compared to a quite scattered response of the RCA biosensor for FET (Figure 5). A quite scattered signal for low-affinity analytes was observed by others, as well, whenELISA-like[41b] and EIS analytical protocols[41] with lectins were applied. This might be caused by a subtle change in the washing protocol in between measurements.

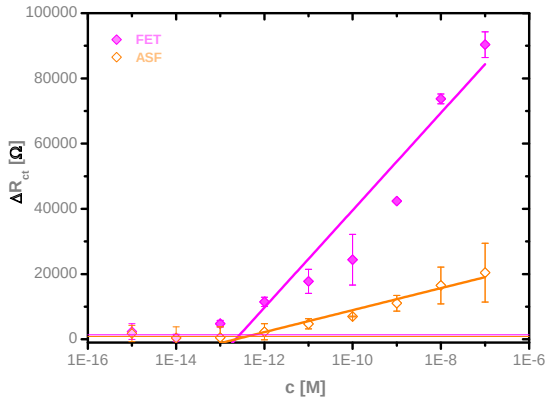

Fig. 4.: Calibration of the SNA biosensor with two glycoproteins (FET: fetuin with 8.7% of N-acetylneuraminic acid, ASF: asialofetuin with 0.5% of N-acetylneuraminic acid). Each analyte was measured at least in triplicate with an independent biosensor device and results are shown with a standard deviation (± SD) calculated in Excel.

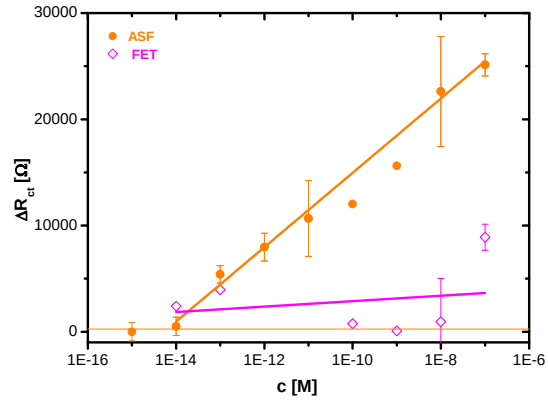

Fig. 5.: Calibration of the RCA biosensor with two glycoproteins (FET: fetuin with 8.7% of N-acetylneuraminic acid, ASF: asialofetuin with 0.5% of N-acetylneuraminic acid). Each analyte was measured at least in triplicate with an independent biosensor device and results are shown with a standard deviation (± SD) calculated in Excel.

Lectin Microarray

The lectin biosensors were validated against a state-of-the-art glycoprofiling tool, a lectin microarray with all lectins used for comparison (Figure S11, Supporting Information). Con A was incubated with three different glycoproteins (INV, oxINV, and TRF) spotted on the chip, and three different concentrations (0.1, 0.01, and 0.001 mg mL−1) were quantified. SNA was incubated with FET and ASF (data not shown due to low signal) spotted; RCA was incubated with FET and ASF spotted at the same concentrations, and results were quantified. Analysis of the lectin microarray was applied for construction of calibration curves, which were compared to calibration curves of all lectin biosensors (Figure 6), indicating that all lectin biosensors offered few orders of magnitude lower detection limits for their analytes and a much wider working concentration range compared to the lectin microarray.

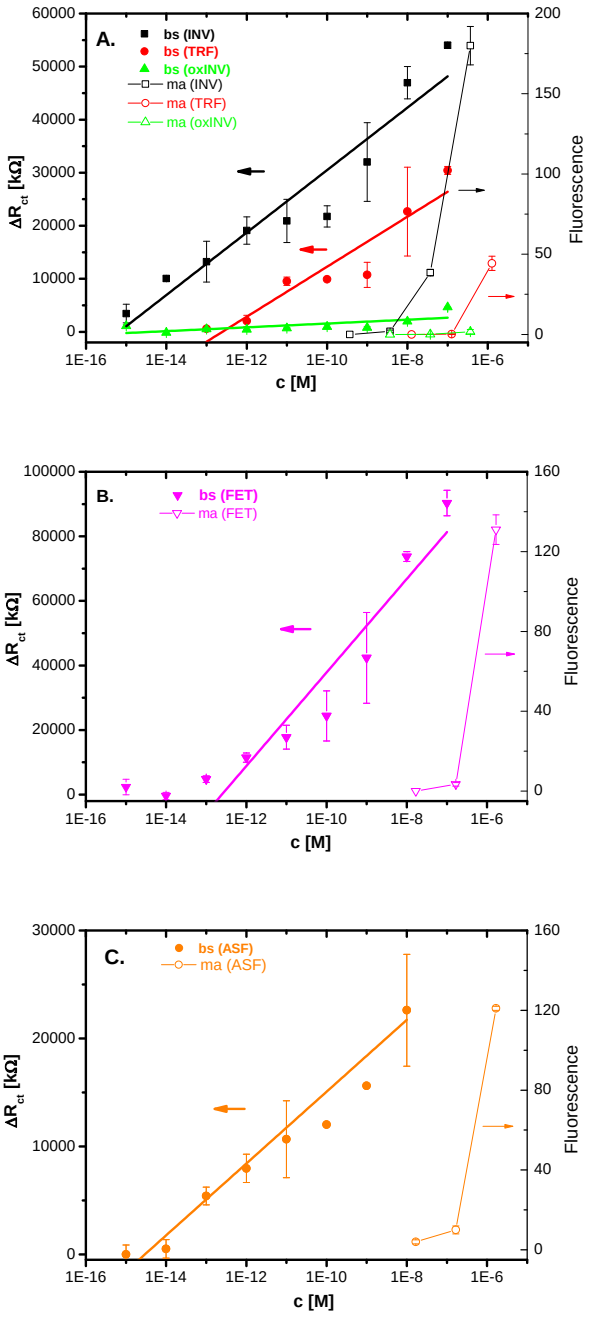

Fig. 6.: A direct comparison of working concentration range for the lectin biosensors (bs) and lectin microarray (ma) applying A) Con A lectin, B) SNA lectin and C) RCA lectin. Each analyte was measured at least in triplicate with an independent biosensor device and results are shown with a standard deviation (± SD) calculated in Excel.

Analysis of Human Samples

Furthermore, the application potential of the lectin biosensors was tested for the analysis of human samples from healthy individuals and from those suffering from rheumatoid arthritis. At first, an optimal dilution of human serum was needed to be found in order to detect glycoproteins with high sensitivity but, at the same time, lowering the effect of nonspecific interactions from such complex samples. A dilution of the human serum samples 1:1000 was selected since, at this dilution, nonspecific response of the sample on the reference surface without any lectin immobilized was negligible, while response with the Con A biosensor was well above nonspecific signal (Figure S12, Supporting Information). The performance of the Con A and SNA biosensors was further validated by standard addition of 1 pM INV and 1 pM FET to human serum diluted 1:1000, respectively. The results showed a recovery of 91% for the Con A biosensor with added INV and of 72% for the SNA biosensor with added FET. A relatively low recovery index for FET might indicate quite quick (1 h of incubation) formation of complexes of FET with other proteins present in human serum via N-acetylneuraminic acid (attached to FET), which is quite often involved in a wide range of interactions within a cell or with other cells, or removal of terminal N-acetylneuraminic acid from FET by sialidases. [10a,42] Thus, the lectin biosensor can be applied for kinetic analysis of the fate of various glycoproteins in complex samples such human serum, which might have physiological consequences. Finally, all three lectin biosensors were applied in the analysis of three human serum samples from healthy individuals and three human serum samples from people affected by rheumatoid arthritis (RA). Circulating antibodies (IgG) in the blood carry complex type glycans of a biantennary structure as shown in the graphical abstract. These biomolecules are hardly ever completed with both N-acetylneuraminic acids present, and in patients with RA, galactose or even Nacetylglucosamine can be exposed.10a The severity of the RA disease tends to correlate with the extent of the glycosylation change.10a Results obtained by the application of the lectin biosensors corroborated prior results that serum samples from healthy individuals had weaker signal on Con A biosensor compared to samples from patients with RA indicating that mannose units are not that exposed on IgG in serum from healthy individuals (Figure 7A). The signal on the RCAbiosensor showed a similar pattern as in the case of the Con A biosensor, suggesting healthy individuals do not have exposed galactose residues available for RCA lectin binding (Figure 7B). The SNA biosensor exhibited higher signals for samples from healthy individuals compared to the RA samples, suggesting in healthy individuals, N-acetylneuraminic acid is still present (Figure 7C). Further experiments are needed to see if lectin biosensors can be applied for the analysis of the severity of RA disease from glycoprofiling of human serum. In order to achieve this goal, the signal from the lectin biosensors has to be correlated with standard clinical methods an effort, which is currently under way.

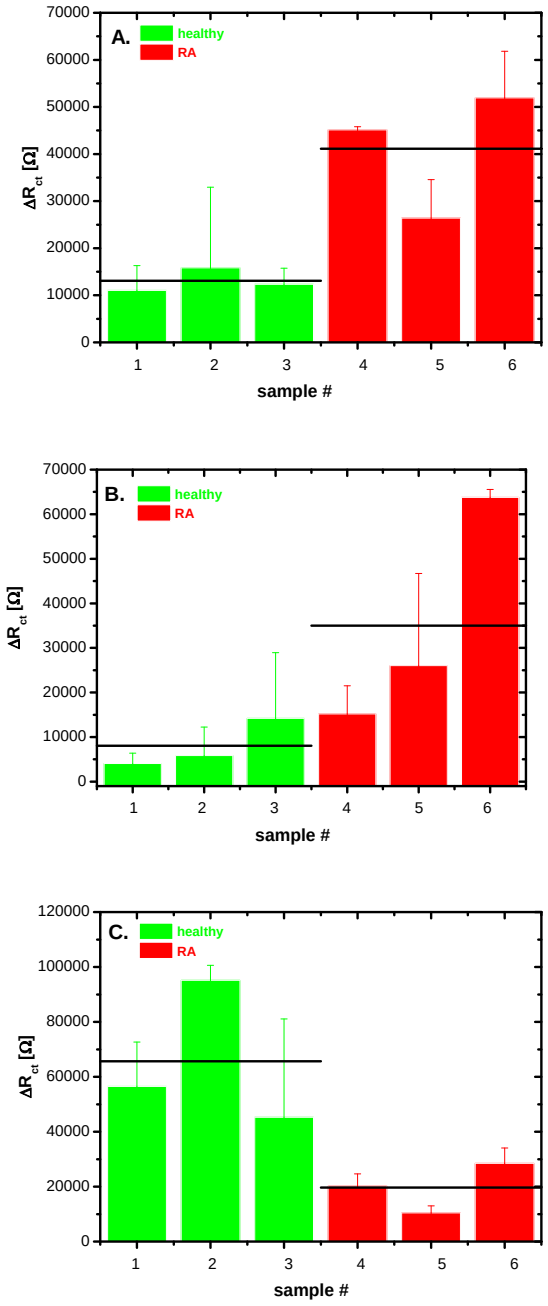

Fig. 7.: Glycoprofile of three human serum samples from healthy individuals and three samples from patients with rheumatoid arthritis (RA) analysed by the A) Con A biosensor, B) RCA biosensor and C) SNA biosensor. Each sample was measured at least in triplicate with an independent biosensor device and results are shown with a standard deviation (± SD) calculated in Excel.

- **Conclusions**

A mixed SAM composed of a newly synthesized thioctic acid derivative DPS and functional thiol MUA provided an interface resisting nonspecific interactions, while allowing covalent immobilization of lectins. The lectin biosensors prepared by immobilization of three different lectins on the gold electrode surface provided high sensitivity of detection of glycoproteins with a detection limit down to the fM level with a wide linear range of operation. The study suggests lectin biosensors outperform lectin microarrays in terms of sensitivity and utilizable working concentration range with a great potential of the lectin biosensors for searching for new disease biomarkers, which can be present in biological samples at extremely low concentrations. Moreover, reliability of biosensing was tested by standard addition with recovery of 91% for INV on the Con A biosensor and 72% for FET on the SNA biosensor. Surprisingly low recovery index for FET on the SNA biosensor might indicate an interaction with serum components via Nacetylneuraminic acid or removal of N-acetylneuraminic acid from the FET by the action of sialidase. Thus, the lectin biosensors can be applied for monitoring of kinetic parameters of interaction of a particular glycoprotein with this sample, which have a diagnostic value. Finally, comparison of a glycoprofile of serum samples from healthy individuals and those having RA showed distinct glycoprofile differences with a potential to detect severity of disease progression in the future.

- **Associated Content**

Supporting Information

Information about electrode pretreatment and SAM formation; human samples; synthesis of sulfobetaine; oxidation of the glycan; experimental procedures (lectin arrays, QCM, XPS, FTIR, and AFM); results from QCM experiments; structure of Con A lectin; structure of glycans on standard glycoproteins; image of a sandwich biosensor configuration; performance of the Con A biosensor built on various SAM interfaces; representative Nyquist plot for the Con A biosensor; raw data from lectin microarray and figure showing optimization of dilution of human sera. This material is available free of charge via the Internet at http://pubs.acs.org.

- **Author Information**

Corresponding Author *E-mail: Jan.Tkac@savba.sk. Tel.: +421 2 5941 0263. Fax: +421 2 5941 0222.

- **Acknowledgments**

The financial support from the Slovak scientific grant agency VEGA 2/0127/10 and from the Slovak research and development agency APVV 0282-11 is acknowledged. The research leading to these results has received funding from the European Research Council under the European Union's Seventh Framework Programme (FP/2007-2013)/ERC Grant Agreement No. 311532.

- **Supplementary information**

Experimental section

Patients and samples

Three (N=3) female patients fulfilling the 2010 ACR-EULAR classification criteria for RA were included in the study.[1] The patients were recruited from a local outpatient rheumatology clinic. Three (N=3) healthy female subjects served as controls. All the studied subjects were non-smokers, had negative history of endocrine disorders, diabetes or impaired glucose tolerance. The RA patients had the following basic clinical characteristics: patient 4 (42 years old, disease duration 31 years, seronegative RA, treatment with methotrexate and hydroxychloroquine), patient 5 (72 years old, disease duration 10 years, seropositive RA, treatment with methotrexate), patient 6 (52 years old, disease duration 1 year, seropositive RA, treatment with prednisone, methotrexate, hydroxychloroquine, nimesulide). All subjects gave informed written consent and the study was approved by the Ethics Committee of the National Institute of Rheumatic Diseases, Piestany, Slovakia in agreement with the ethical guidelines of the Declaration of Helsinki as revised in 2000. Blood samples were taken into standard serum tubes with silicone-coated interior (BD Vacutainer, Franklin Lakes, NJ USA), clotted at room temperature for approximately one hour, and subsequently the serum was transferred into separate tubes and stored at -20°C. Before analyses, the human serum samples were diluted by 10 mM PBS buffer pH 7.4. All stock solutions (lectins, standard glycoproteins and human sera) were stored at -20 °C in aliquots.

Synthesis of (R)-3-((2-(5-(1,2-dithiolan-3-yl)pentanamido)ethyl)dimethylammonio)propane-1-sulfonate

A new thioctic derivative (*R*)-3-((2-(5-(1,2-dithiolan-3-yl)pentanamido)ethyl) dimethylammonio)propane-1-sulfonate used in the SAM preparation was synthesized in two steps (Scheme 1). The first step is preparation of (*R*)-*N*-(2-(dimethylamino)ethyl)-5-(1,2-dithiolan-3-yl)pentanamide[2] as follows: To a stirred solution of (*R*)-Lipoid acid (2.00 g, 9.69 mmol) in CH_2Cl_2 (80.0 mL) and added dropwise DCC (2.40 g, 11.60 mmol, 1.2 equiv) dissolved in dried dichloromethane (4.0 mL) . The resulting mixture was stirred for 30 min at room temperature. A solution of *N*-hydroxysuccinimide (NHS, 1.34 g, 11.60 mmol, 1.2 equiv) in acetonitrile (2.0 mL) was added. After stirring for 30 min at room temperature, *N*,*N*-dimethylethylene diamine (3.20 mL, 29.10 mmol, 3.0 equiv) was added dropwise and the reaction was stirred overnight at room temperature. Reaction mixture (yellowish fine suspension) was filtered with the aid of CH_2Cl_2 (15 mL). The filtrate was washed three times with an aqueous solution of 1 M NaOH (3 x 35 mL) and 1 M NaCl (3 x 35 mL), dried (Na_2SO_4), filtered and evaporated under a reduced pressure. Resulting dense oil was dissolved in 1 M HCl (80 mL) and stirred for an hour, filtered and the aqueous solution was added to $CHCl_3$ chloroform (100 mL). The pH was adjusted to 12-13 with NaOH and the two phase system was mixed thoroughly for 30 min. The phases were separated, and the aqueous layer was twice extracted by $CHCl_3$ (2 x 40 mL). Cysteine (10 mg) was added to a combined organic extracts. Organic extracts were dried (Na_2SO_4), filtered and concentrated under a reduced pressure, to give titled compound as a dense yellow oil (2.00 g, 75%). Note: The product can be stored at -20 °C. The product was characterised by IR and NMR with the following characteristics: **IR** (ATR) 3297, 2933, 2769, 1643 (s, NCO), 1550, 1458, 1252, 1042, 752 cm^{-1}; **^{1}H NMR** (400 MHz, $CDCl_3$) δ 6.04 (br s, 1H, NH), 3.56 (m, 1H, H-C3), 3.31 (2 x t, *J* = 5.5 Hz, 2H, HN-CH_2-CH_2), 3.24 – 3.02 (m, 2H, CH_2-5), 2.90 – 2.68 (m, 2H, CH_2-CH_2-NMe_2), 2.56 – 2.34 (m, 3H, H^a-4 and CH_2-2'), 2.22 (s, 6H, NMe_2), 1.93 (3, 1H, H^a-4), 1.80 – 1.54 (m, 4H, CH_2-3' and CH_2-5'), 1.54 – 1.34 (m, 2H, CH_2-4') ppm.

The second step was preparation of (R)-3-((2-(5-(1,2-dithiolan-3-yl)pentanamido)ethyl)dimethylammonio)propane-1-sulfonate (DPS), as follows. To a stirred solution of (*R*)-*N*-(2-(dimethylamino)ethyl)-5-(1,2-dithiolan-3-yl)pentanamide (1.10 g, 4.00 mmol) in dried THF (6.0 mL) was added dropwise solution 1,3-propane sultone (540 mg, 4.40 mmol, 1.10 equiv) in dried THF (2.0 mL) under argon atmosphere and the reaction mixture was stirred overnight at room temperature. Formed white suspension was centrifuged (3045 g, 5 min) and a supernatant was discarded. A residue was triturated with diethyl ether, acetone and the product was dried under a reduced pressure, to give DPS (see Scheme 1) as a white solid (1.10g, 70%). The product was characterised by IR and NMR with the following characteristics: **IR** (FTIR) 3460, 3296, 2978, 2868, 1655 (s, NCO), 1544, 1445, 1184, 1037, 730 cm^{-1}; **^{1}H NMR** (400 MHz, D_2O) δ 3.75 (m, 1H, NH-CH_2-), 3.65 – 3.46 (m, 6H, NH-CH_2- and H-3 and CH_2-N^+ and N^+-CH_2), 3.35 – 3.21 (m, 2H, H-5), 3.20 (s, 6H, N^+Me_2), 3.01 (t, *J* = 7.2 Hz, 2H, CH_2-SO_3^-), 2.53 (m, 1H, H-4), 2.44 – 2.18 (m, 4H, H-2' and CH_2-CH_2-$CH_2SO_3^-$), 2.03 (m, 1H, H-4), 1.83 – 1.56 (m, 4H, H-3'and H-5'), 1.54 – 1.37 (m, 2H, H-4') ppm; **^{13}C NMR** (100.6 MHz, D_2O) δ 177.05 (NCO), 62.93 (CH_2-CH_2-N^+), 61.81 (CH_2-CH_2-N^+), 56.65 (C-3), 51.27 (Me-N^+), 51.09 (Me-N^+), 47.31 (CH_2), 40.43 (CH_2, C-4), 38.36 (CH_2, C-5), 35.43 (CH_2), 33.93 (CH_2), 33.15 (CH_2), 28.15 (CH_2), 24.92 (CH_2), 18.32 (CH_2) ppm.

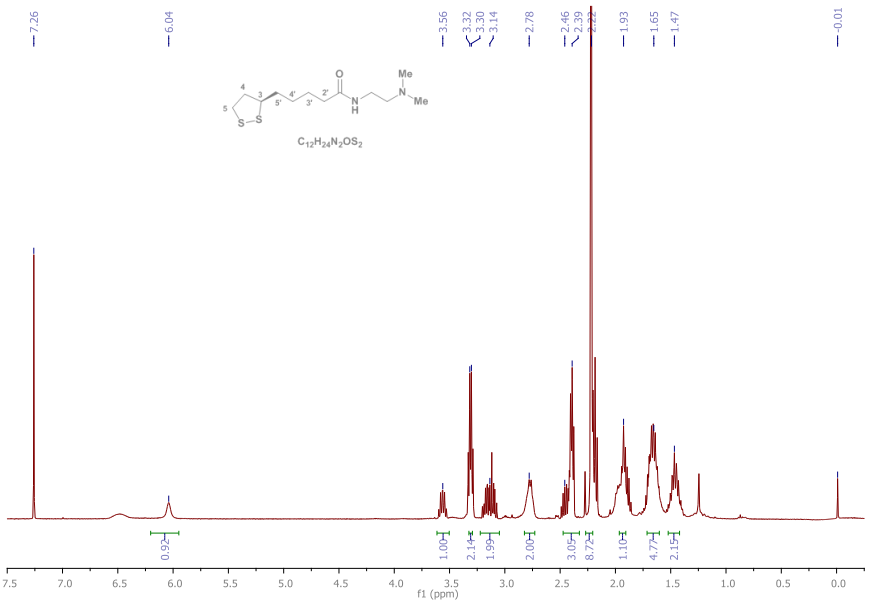

^{1}H NMR spectrum of *(R)*-*N*-(2-(dimethylamino)ethyl)-5-(1,2-dithiolan-3-yl)pentanamide.

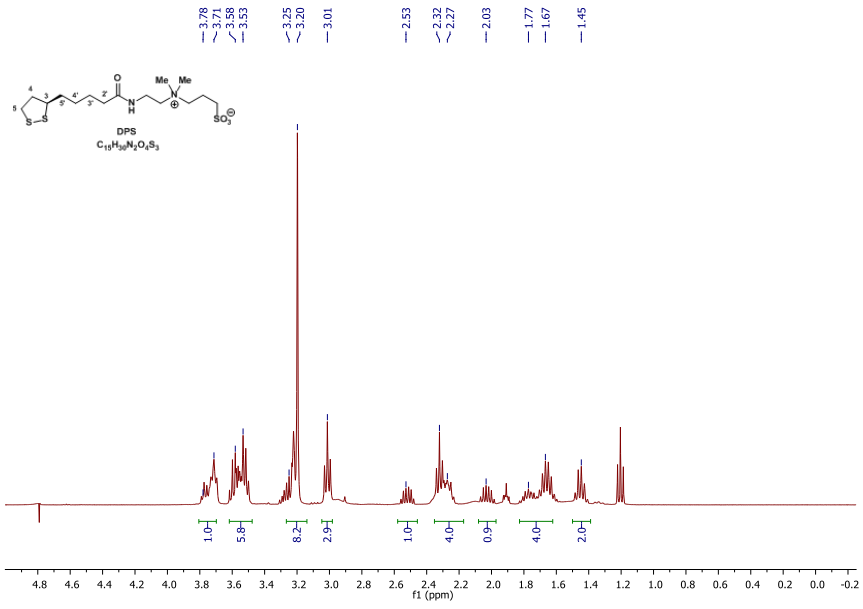

^{1}H NMR spectrum of DPS.

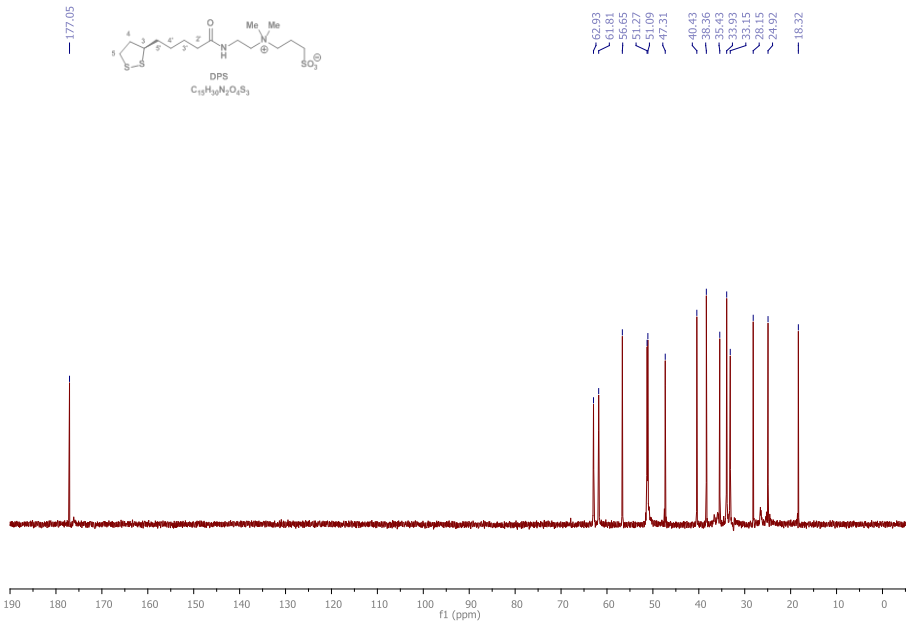

^{13}C NMR spectrum of DPS.

Oxidation of the glycan moieties on glycoproteins

Glycan structures in INV were chemically oxidised using sodium periodate according to protocol described earlier.[3] Shortly, 10 μM of stock solution of INV was oxidised by 10 mM sodium periodate in 50% acetonitrile solution for 2 h in dark at a laboratory temperature. Reaction was stopped by an addition of ethyleneglycol to a final concentration of 15% (v/v) and incubated for additional hour in dark. Free aldehyde groups formed by glycan oxidation, verified by FTIR (data not shown), were blocked by incubation with 1 mM ethanolamine for 1 h in dark and finally the oxidised INV (oxINV) was recovered with a desalting column.

Lectin microarray assays

For lectin microarray experiments, a printing buffer (11.3 mM NaH_2PO_4, 9 mM KOH, 137 mM NaCl, pH 7.4), a washing buffer (printing buffer containing 0.05% (v/v) Tween-20, pH 7.4), and a blocking and binding buffer (washing buffer + 1 M ethanolamine) were used. Five different concentrations of four different glycoproteins (INV, oxINV, FET and TRF) were spotted using SpotBot3 Microarray Protein edition (Arrayit, USA) on an epoxide coated slides Nexterion E (Schott, Germany) using a previously optimised protocol at temperature of 10 °C and humidity of 50 %.[4] The highest glycoprotein concentration investigated was 0.1 mg ml^{-1}. After glycoprotein printing, the slide was incubated with a blocking buffer in the humidity chamber for 1 h at a room temperature with humidity of 80 % with a slow shaking. The slide was gently rinsed by a printing buffer in a Petri dish, drained to remove an excess of a buffer and then, 70 μl of a 50 □g ml^{-1} biotinylated lectins solutions (Con A and SNA) in a binding buffer were dropped on the slide surface and incubated for 1 h. After incubation, the slide was incubated with the CF555-streptavidin solution (5 μg ml^{-1} in a binding buffer) for 15 min. After washing, the slide was scanned using InnoScan710 scanner (Innopsys, France) at the wavelength of 532 nm. The slide image was evaluated using the Mapix 5.5.0 software and slide image was evaluated in Photo-PAINT X5 software (Corel, USA) by evaluation of the intensity of green spots (484 pixels) with a black colour having a value of 0 and a green one having a value of 255. Intensity of eight independent array spots was evaluated for every glycoprotein analysed.

Quartz crystal microbalance (QCM) measurements

All QCM measurements were performed with Autolab PGSTAT 128N (Ecochemie, Netherlands) equipment using an optional EQCM module. The changes of a mass were evaluated using Sauerbrey´s equation:

$$\Delta f = -\frac{2f_0^2}{A\sqrt{\rho_q \mu_q}}.\Delta m \qquad \text{(eqn. 1)},$$

where Δf is the frequency change (Hz), f_0 is the nominal resonant frequency of the crystal (6 MHz), Δm is the change in mass (g cm^{-2}) and μ_q is the shear modulus of a quartz (g cm^{-1} s^{-2}), A is the surface area and □$_q$ is density of quartz in g ml^{-1} . For a 6 MHz crystal, the whole equation can be simplified to:

$$\Delta f = -C_f.\Delta m \qquad \text{(eqn. 2)},$$

where C_f is a frequency constant 0.0815 Hz ng^{-1} cm^2. The measurements were monitored and evaluated using the Nova 1.9 software and all measurements were run at room temperature.

X-ray photoelectron spectroscopy (XPS) measurements

The XPS signals on square shaped gold chips (Litcon, Sweden) of 12x12x0.3 mm modified as previously described[5] for SAM formation

on gold electrodes were recorded using a Thermo Scientific K-Alpha XPS system (Thermo Fisher Scientific, UK) equipped with a micro-focused, monochromatic Al Kα X-ray source (1486.6 eV). An X-ray beam of 400 μm size was used at 6 mA x 12 kV. The spectra were acquired in the constant analyser energy mode with pass energy of 200 eV for the survey. Narrow regions were collected with pass energy of 50 eV. Charge compensation was achieved with the system flood gun that provides low energy electrons (~0 eV) and low energy argon ions (20 eV) from a single source. The argon partial pressure was $2x10^{-7}$ mbar in the analysis chamber. The Thermo Scientific *Avantage* software, version 4.84 (Thermo Fisher Scientific), was used for digital acquisition and data processing. Spectral calibration was determined by using the automated calibration routine and the internal Au, Ag and Cu standards supplied with the K-Alpha system. The surface compositions (in atomic %) were determined by considering the integrated peak areas of detected atoms and the respective sensitivity factors.

Fourier-transform infrared (FTIR) spectroscopy

Fourier-transform infra red (FTIR) spectra were measured with Nicolet 6700 (Thermo Fisher Scientific, USA) spectrometer equipped with DTGS detector and Omnic 8.0 software. The spectra were collected in the middle region from 4,000 to 400 cm^{-1} at a resolution of 4 cm^{-1}, the number of scans was 128. Diamond Smart Orbit ATR accessory was applied for measurement in a solid state.

Atomic force microscopy (AFM)

Peak force tapping mode atomic force microscopy (Scan Asyst, Bruker, USA) in air was carried out on a Bioscope Catalyst instrument and Olympus IX71 microscope in conjunction with NanoScope 8.15 software at a scan rate 0,5 line s^{-1} with the tip set of 200 pN. Square shaped gold chips (12x12x0.3 mm) were modified as previously described for the planar gold electrodes and scanned using SCANASYST-AIR silicon tip on nitride lever (Bruker, USA, with f_0=50-90 kHz and k=0.4 N m^{-1}), sharpened for a tip radius of 2 nm.

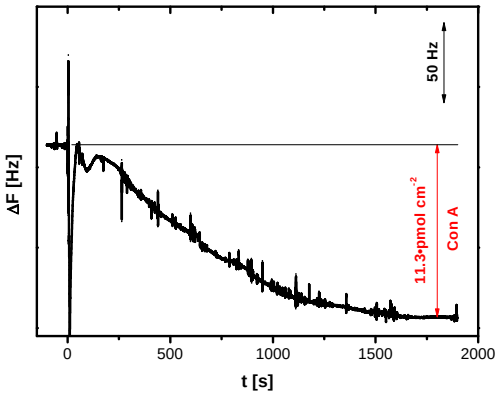

Fig. S1.: Quartz crystal microbalance experiment showing immobilisation of Con A lectin injected at time t=0 s on a SAM layer deposited from a 1+1 mixture of betaine and 11-mercaptoundecanoic acid.

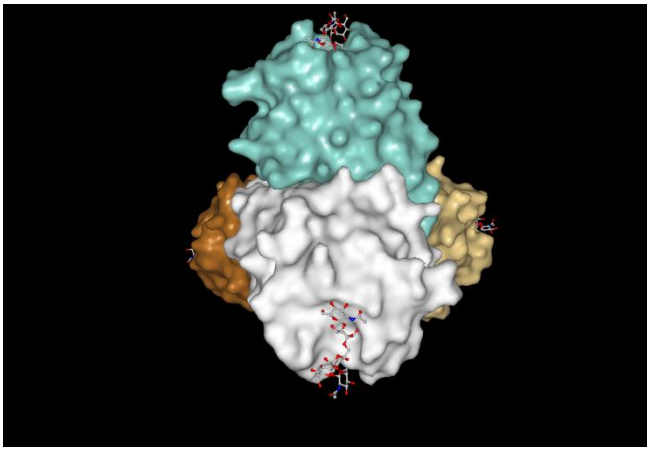

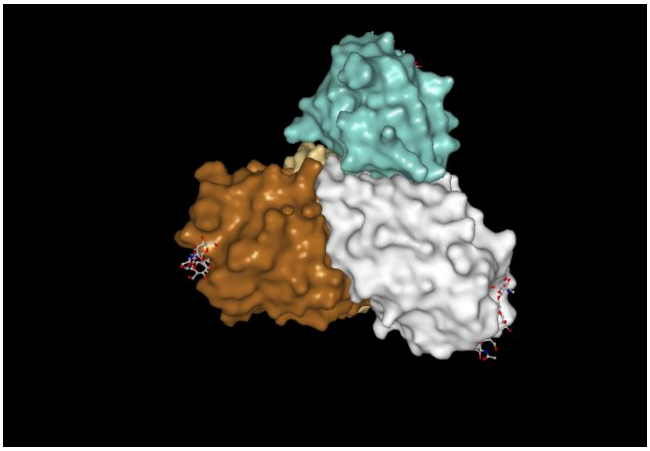

Fig. S2.: Structure of Con A lectin (PDB file 1TEI) showing composition from four identical subunits, which are represented in different colours.

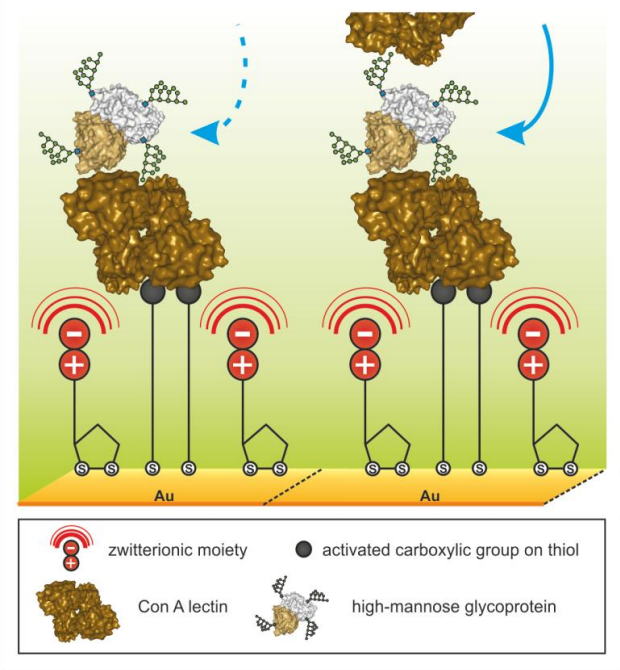

Fig. S3.: Schematic representation of the Con A biosensor after biorecognition took place (on the left) and the sandwich configuration of the Con A biosensor with additional outer layer of Con A lectin.

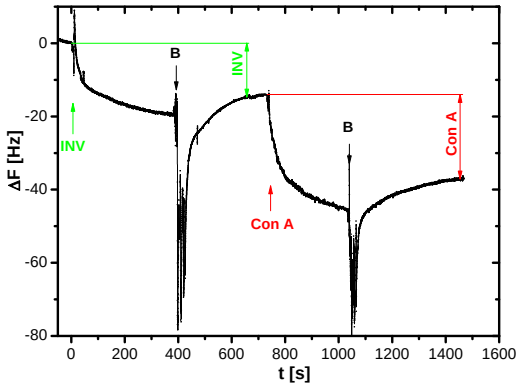

Fig. S4.: Quartz crystal microbalance assay showing that the Con A biosensor after interaction with its analyte invertase (INV) is able to interact with Con A lectin forming additional outer lectin layer (see Fig. S3 for graphical represenataion).

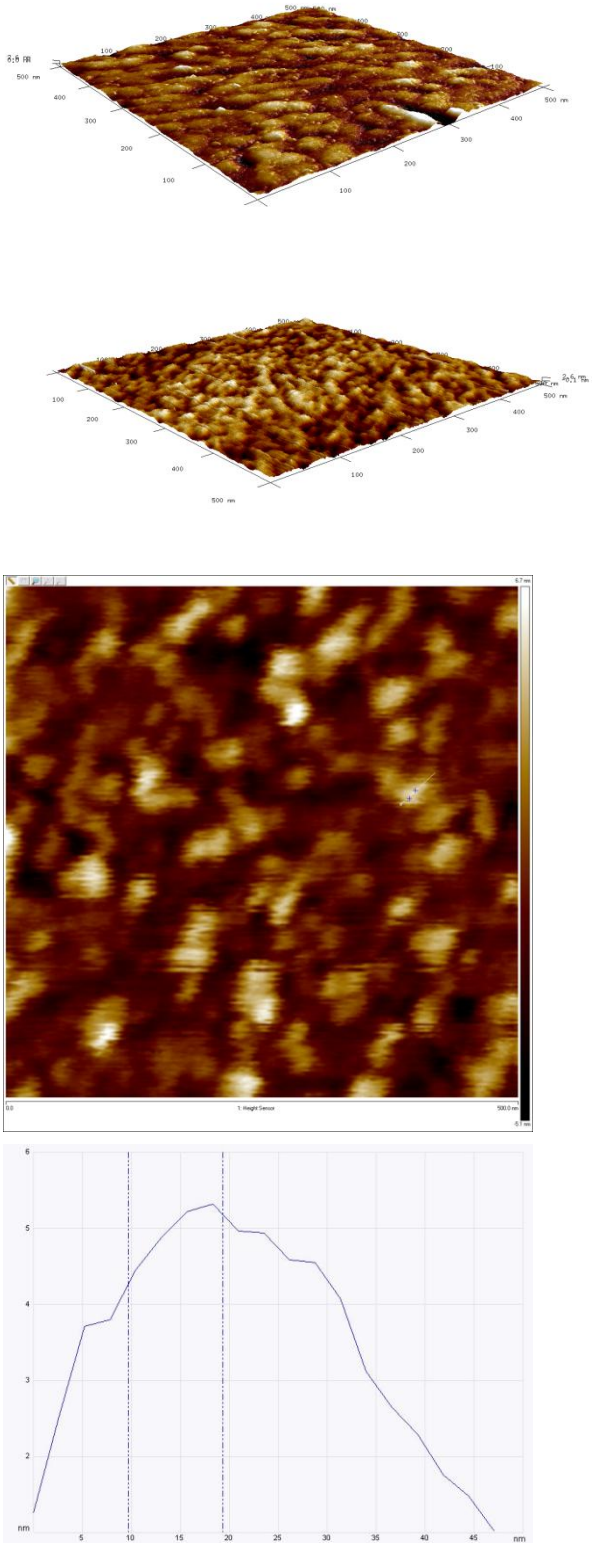

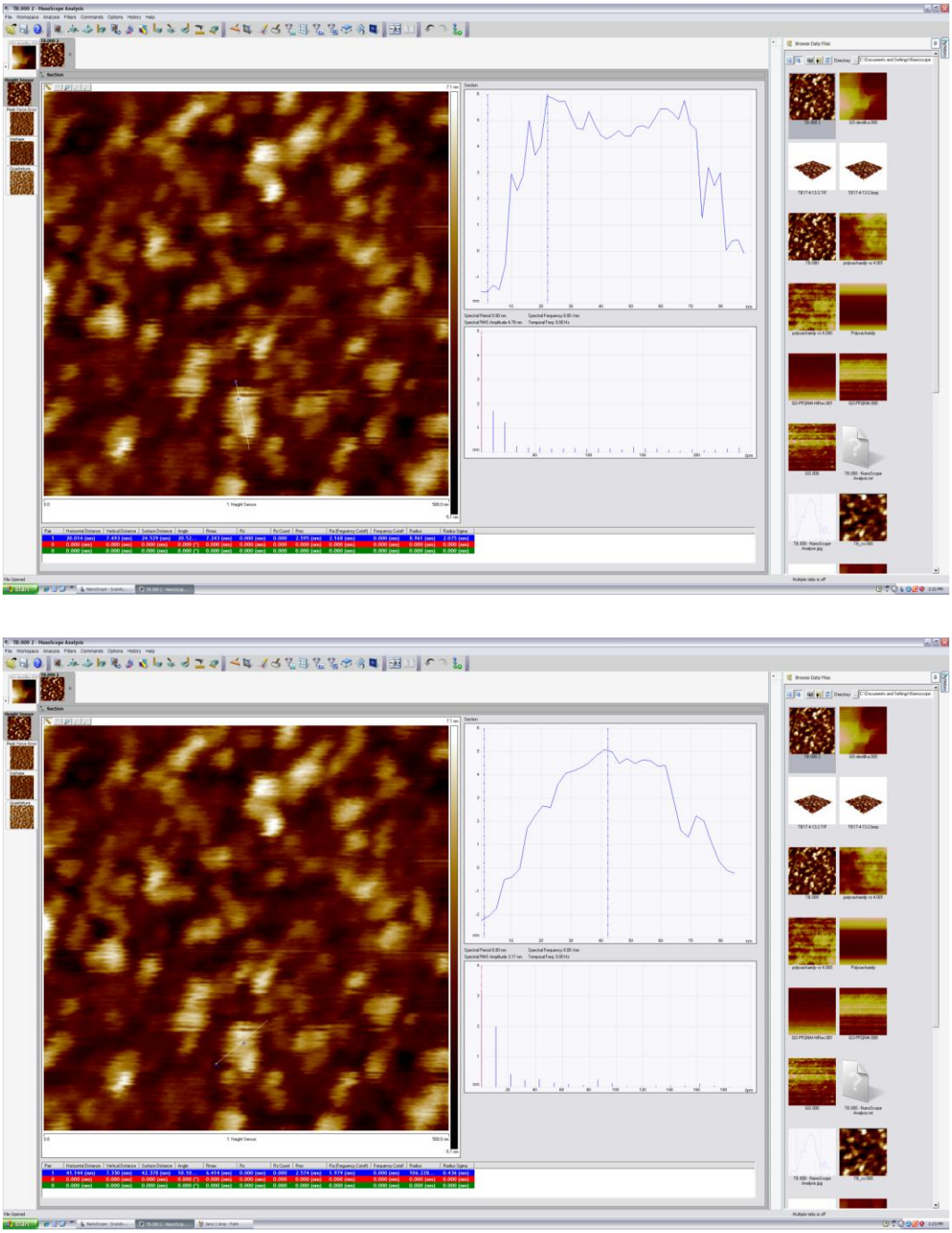

Fig. S5.: AFM images of bare gold surface (upper row on left), gold surface modified by SAM (upper row on right), and larger Con A spots on the surface after Con A immobilisation.

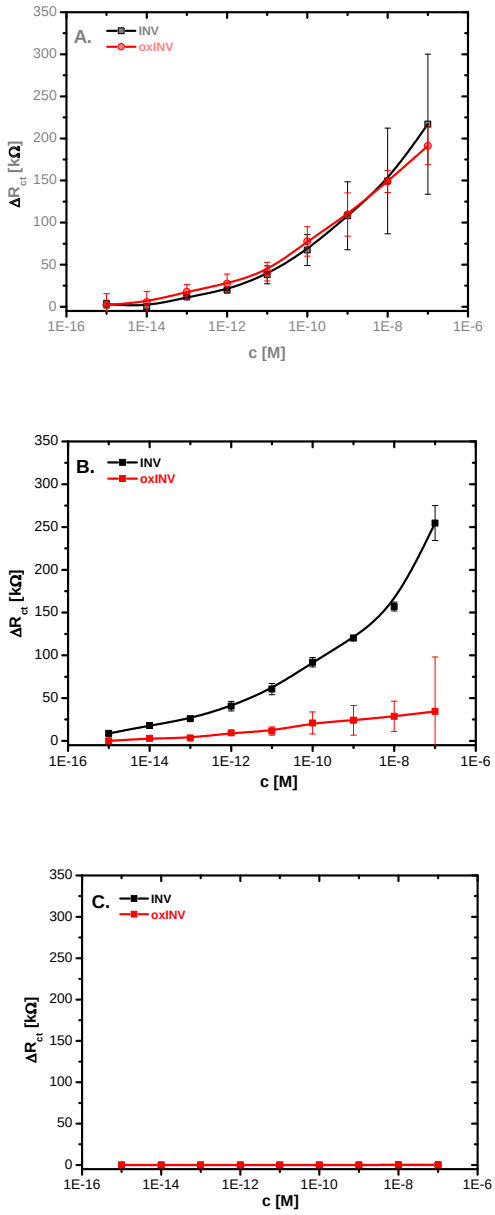

Fig. S6.: Calibration curves for the Con A biosensor built on SAM layer deposited from a mixture 11-mercaptoundecanoic acid: betaine of A) 3+1, B) 1+3 and C) 0+1 i.e. a pure betaine SAM layer.

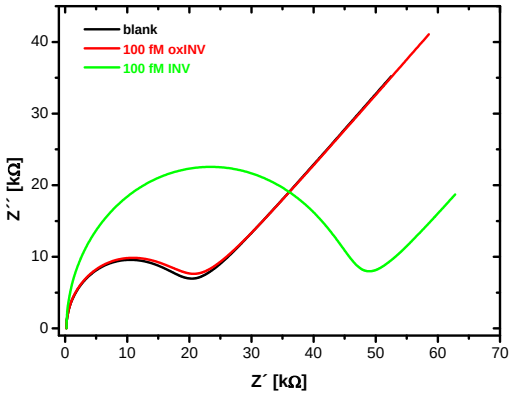

Fig. S7.: A typical Nyquist plot of the Con A biosensor incubated with its analyte invertase (INV) and oxidised invertase (oxINV) applied as a control. Moreover, the response of the Con biosensor in a plain PBS buffer is shown, as well.

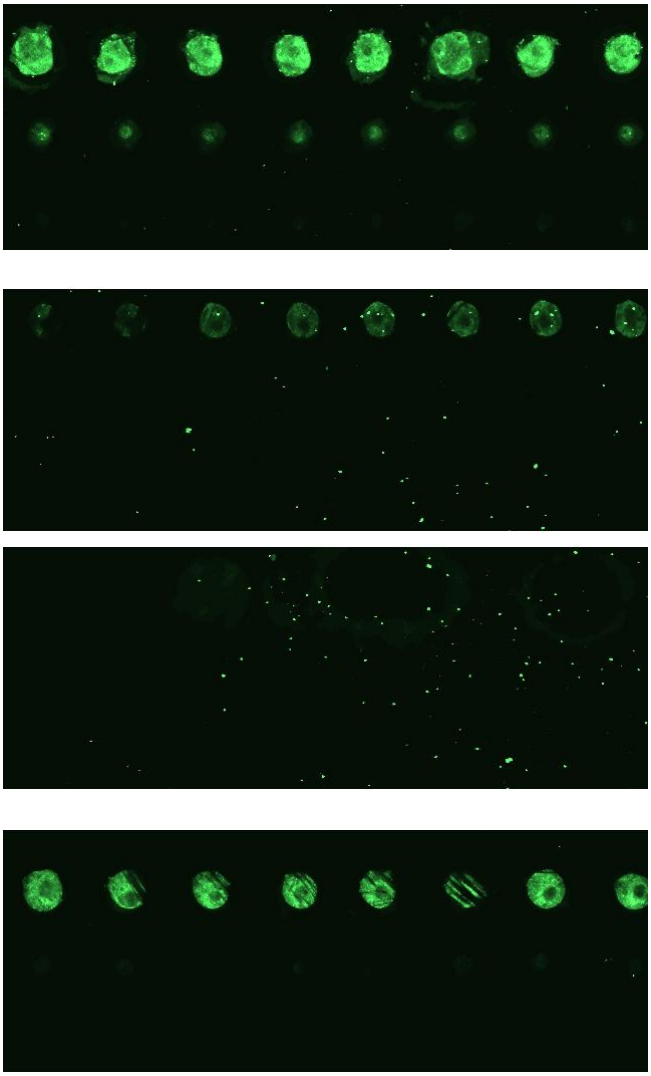

Fig. S8.: Application of the lectin microarray in analysis of various glycoproteins printed at three different concentrations (in every image upper row - 1 mg ml^{-1}, middle row – 0.1 mg ml^{-1} and lower row – 0.01 mg ml^{-1}). Upper left image shows interaction of Con A with invertase, upper right image Con A interaction with transferrin, lower left image Con A with oxidised invertase and lower right image interaction of SAN lectin with fetuin.

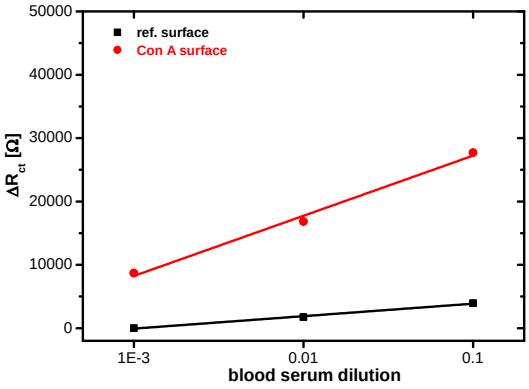

Fig. S9.: Optimisation of a dilution of blood serum in order to get sensitive glycoprofiling by the biosensor, while minimising non-specific interactions.

(1) Aletaha, D.; Neogi, T.; Silman, A. J.; Funovits, J.; Felson, D. T.; Bingham, C. O.; Birnbaum, N. S.; Burmester, G. R.; Bykerk, V. P.; Cohen, M. D.; Combe, B.; Costenbader, K. H.; Dougados, M.; Emery, P.; Ferraccioli, G.; Hazes, J. M.; Hobbs, K.; Huizinga, T. W.; Kavanaugh, A.; Kay, J.; Kvien, T. K.; Laing, T.; Mease, P.; Ménard, H. A.; Moreland, L. W.; Naden, R. L.; Pincus, T.; Smolen, J. S.; Stanislawska-Biernat, E.; Symmons, D.; Tak, P. P.; Upchurch, K. S.; Vencovský, J.; Wolfe, F.; Hawker, G. *Annals of the Rheumatic Diseases* **2010**, *69*, 1580.
(2) Lawrence, L. J.; Eisenberg, R. L. *US 2007/0083054 A1* **2005**, *11/248,358*.
(3) Li, Y.; Tian, Y.; Rezai, T.; Prakash, A.; Lopez, M. F.; Chan, D. W.; Zhang, H. *Analytical Chemistry* **2010**, *83*, 240.
(4) Bertok, T.; Sediva, A.; Katrlik, J.; Gemeiner, P.; Mikula, M.; Nosko, M.; Tkac, J. *Talanta* **2013**, *108*, 11.
(5) Bertok, T.; Gemeiner, P.; Mikula, M.; Gemeiner, P.; Tkac, J. *Microchimica Acta* **2013**, *180*, 151.

- **References**

(1) Schena, M.; Shalon, D.; Davis, R. W.; Brown, P. O. *Science* **1995**, *270*, 467.

(2) Eisen, M. B.; Spellman, P. T.; Brown, P. O.; Botstein, D. *Proceedings of the National Academy of Sciences* **1998**, *95*, 14863.

(3) Alizadeh, A. A.; Eisen, M. B.; Davis, R. E.; Ma, C.; Lossos, I. S.; Rosenwald, A.; Boldrick, J. C.; Sabet, H.; Tran, T.; Yu, X.; Powell, J. I.; Yang, L.; Marti, G. E.; Moore, T.; Hudson, J.; Lu, L.; Lewis, D. B.; Tibshirani, R.; Sherlock, G.; Chan, W. C.; Greiner, T. C.; Weisenburger, D. D.; Armitage, J. O.; Warnke, R.; Levy, R.; Wilson, W.; Grever, M. R.; Byrd, J. C.; Botstein, D.; Brown, P. O.; Staudt, L. M. *Nature* **2000**, *403*, 503.

(4) Gygi, S. P.; Rochon, Y.; Franza, B. R.; Aebersold, R. *Molecular and Cellular Biology* **1999**, *19*, 1720.

(5) Gry, M.; Rimini, R.; Stromberg, S.; Asplund, A.; Ponten, F.; Uhlen, M.; Nilsson, P. *BMC Genomics* **2009**, *10*, 365.

(6) (a) MacBeath, G.; Schreiber, S. L. *Science* **2000**, *289*, 1760(b) Zhu, H.; Snyder, M. *Current Opinion in Chemical Biology* **2003**, *7*, 55(c) Lee, J.-R.; Magee, D. M.; Gaster, R. S.; LaBaer, J.; Wang, S. X. *Expert Review of Proteomics* **2013**, *10*, 65(d) Rusmini, F.; Zhong, Z.; Feijen, J. *Biomacromolecules* **2007**, *8*, 1775.

(7) Jenuwein, T.; Allis, C. D. *Science* **2001**, *293*, 1074.

(8) Jeffrey, P. D.; Russo, A. A.; Polyak, K.; Gibbs, E.; Hurwitz, J.; Massague, J.; Pavletich, N. P. *Nature* **1995**, *376*, 313.

(9) Arnaud, J.; Audfray, A.; Imberty, A. *Chemical Society Reviews* **2013**.

(10) (a) Varki, A. *Essentials of glycobiology*; Cold Spring Harbor Laboratory Press: Cold Spring Harbor, N.Y., 2009(b) Bertók, T.; Katrlík, J.; Gemeiner, P.; Tkac, J. *Microchimica Acta* **2013**, *180*, 1.

(11) (a) Gemeiner, P.; Mislovicová, D.; Tkác, J.; Svitel, J.; Pätoprstı, V.; Hrabárová, E.; Kogan, G.; Kozár, T. *Biotechnology Advances* **2009**, *27*, 1(b) Katrlík, J.; Švitel, J.; Gemeiner, P.; Kožár, T.; Tkac, J. *Medicinal Research Reviews* **2010**, *30*, 394(c) Hirabayashi, J. *Nat Chem Biol* **2009**, *5*, 198(d) Krishnamoorthy, L.; Bess, J. W.; Preston, A. B.; Nagashima, K.; Mahal, L. K. *Nat Chem Biol* **2009**, *5*, 244(e) Schauer, R.; Kamerling, J. P. *ChemBioChem* **2011**, *12*, 2246(f) Song, X.; Lasanajak, Y.; Xia, B.; Heimburg-Molinaro, J.; Rhea, J. M.; Ju, H.; Zhao, C.; Molinaro, R. J.; Cummings, R. D.; Smith, D. F. *Nat Meth* **2011**, *8*, 85(g) Vaishnava, S.; Yamamoto, M.; Severson, K. M.; Ruhn, K. A.; Yu, X.; Koren, O.; Ley, R.; Wakeland, E. K.; Hooper, L. V. *Science* **2011**, *334*, 255.

(12) (a) Burton, D. R.; Poignard, P.; Stanfield, R. L.; Wilson, I. A. *Science* **2012**, *337*, 183(b) Doores, K. J.; Fulton, Z.; Hong, V.; Patel, M. K.; Scanlan, C. N.; Wormald, M. R.; Finn, M. G.; Burton, D. R.; Wilson, I. A.; Davis, B. G. *Proceedings of the National Academy of Sciences* **2010**, *107*, 17107(c) Pejchal, R.; Doores, K. J.; Walker, L. M.; Khayat, R.; Huang, P.-S.; Wang, S.-K.; Stanfield, R. L.; Julien, J.-P.; Ramos, A.; Crispin, M.; Depetris, R.; Katpally, U.; Marozsan, A.; Cupo, A.; Maloveste, S.; Liu, Y.; McBride, R.; Ito, Y.; Sanders, R. W.; Ogohara, C.; Paulson, J. C.; Feizi, T.; Scanlan, C. N.; Wong, C.-H.; Moore, J. P.; Olson, W. C.; Ward, A. B.; Poignard, P.; Schief, W. R.; Burton, D. R.; Wilson, I. A. *Science* **2011**, *334*, 1097.

(13) (a) Anthony, R. M.; Kobayashi, T.; Wermeling, F.; Ravetch, J. V. *Nature* **2011**, *475*, 110(b) Anthony, R. M.; Nimmerjahn, F.; Ashline, D. J.; Reinhold, V. N.; Paulson, J. C.; Ravetch, J. V. *Science* **2008**, *320*, 373(c) Klein, F.; Halper-Stromberg, A.; Horwitz, J. A.; Gruell, H.; Scheid, J. F.; Bournazos, S.; Mouquet, H.; Spatz, L. A.; Diskin, R.; Abadir, A.; Zang, T.; Dorner, M.; Billerbeck, E.; Labitt, R. N.; Gaebler, C.; Marcovecchio, P. M.; Incesu, R.-B.; Eisenreich, T. R.; Bieniasz, P. D.; Seaman, M. S.; Bjorkman, P. J.; Ravetch, J. V.; Ploss, A.; Nussenzweig, M. C. *Nature* **2012**, *492*, 118(d) Li, F.; Ravetch, J. V. *Science* **2011**, *333*, 1030(e) Kim, J.-H.; Resende, R.; Wennekes, T.; Chen, H.-M.; Bance, N.; Buchini, S.; Watts, A. G.; Pilling, P.; Streltsov, V. A.; Petric, M.; Liggins, R.; Barrett, S.; McKimm-Breschkin, J. L.; Niikura, M.; Withers, S. G. *Science* **2013**, *340*, 71.

(14) (a) Kim, E. H.; Misek, D. E. *International Journal of Proteomics* **2011**, *2011*(b) Ferens-Sieczkowska, M.; Kowalska, B.; Kratz, E. M. *Biomarkers* **2013**, *18*, 10(c) Chandler, K. B.; Goldman, R. *Molecular & Cellular Proteomics* **2013**(d) Gilgunn, S.; Conroy, P. J.; Saldova, R.; Rudd, P. M.; O'Kennedy, R. J. *Nat Rev Urol* **2013**, *10*, 99.

(15) (a) Beck, A.; Sanglier-Cianférani, S.; Van Dorsselaer, A. *Analytical Chemistry* **2012**, *84*, 4637(b) Schmaltz, R. M.; Hanson, S. R.; Wong, C.-H. *Chemical Reviews* **2011**, *111*, 4259(c) van Bueren, J. J. L.; Rispens, T.; Verploegen, S.; van der Palen-Merkus, T.; Stapel, S.; Workman, L. J.; James, H.; van Berkel, P. H. C.; van de Winkel, J. G. J.; Platts-Mills, T. A. E.; Parren, P. W. H. I. *Nat Biotech* **2011**, *29*, 574.

(16) Beck, A.; Reichert, J. M. *mAbs* **2012**, *4*, 419.

(17) Raman, R.; Raguram, S.; Venkataraman, G.; Paulson, J. C.; Sasisekharan, R. *Nat Meth* **2005**, *2*, 817.

(18) Gabius, H.-J.; André, S.; Jiménez-Barbero, J.; Romero, A.; Solís, D. *Trends in biochemical sciences* **2011**, *36*, 298.

(19) Cummings, R. D. *Molecular BioSystems* **2009**, *5*, 1087.

(20) Bertozzi, C. R.; Kiessling; L., L. *Science* **2001**, *291*, 2357.

(21) (a) Furukawa, J.-i.; Fujitani, N.; Shinohara, Y. *Biomolecules* **2013**, *3*, 198(b) Rakus, J. F.; Mahal, L. K. *Annual Review of Analytical Chemistry* **2011**, *4*, 367(c) Smith, D. F.; Cummings, R. D. *Molecular & Cellular Proteomics* **2013**.

(22) (a) Oliveira, C.; Teixeira, J. A.; Domingues, L. *Critical Reviews in Biotechnology* **2013**, *33*, 66(b) Murphy, P.; André, S.; Gabius, H.-J. *Molecules* **2013**, *18*, 4026.

(23) (a) Mislovičová, D.; Katrlík, J.; Paulovičová, E.; Gemeiner, P.; Tkac, J. *Colloids and Surfaces B: Biointerfaces* **2012**, *94*, 163(b) Mislovičová, D.; Gemeiner, P.; Kozarova, A.; Kožár, T. *Biologia* **2009**, *64*, 1.

(24) (a) Hirabayashi, J.; Kuno, A.; Tateno, H. *ELECTROPHORESIS* **2011**, *32*, 1118(b) Hirabayashi, J.; Yamada, M.; Kuno, A.; Tateno, H. *Chemical Society Reviews* **2013**(c) Krishnamoorthy, L.; Mahal, L. K. *ACS Chemical Biology* **2009**, *4*, 715.

(25) (a) Reuel, N. F.; Mu, B.; Zhang, J.; Hinckley, A.; Strano, M. S. *Chemical Society Reviews* **2012**, *41*, 5744(b) Q.;, G. J.; Stephen;, C.; Marian;, K.; Lokesh;, J. *Biochemical Society Transactions* **2010**, *38*, 1333(c) Cunningham, S.; Gerlach, J. Q.; Kane, M.; Joshi, L. *Analyst* **2010**, *135*, 2471(d) Sanchez-Pomales , G.; Zangmeister, R. A. *International Journal of Electrochemistry* **2011**, *2011*(e) Reuel, N. F.; Ahn, J.-H.; Kim, J.-H.; Zhang, J.; Boghossian, A. A.; Mahal, L. K.; Strano, M. S. *Journal of the American Chemical Society* **2011**, *133*, 17923(f) Tkac, J.; Davis, J. J. In *Engineering the Bioelectronic Interface: Applications to Analyte Biosensing and Protein Detection* Davis, J. J., Ed.; Royal Society of Chemistry: Cambridge, 2009.

(26) (a) Bertok, T.; Gemeiner, P.; Mikula, M.; Gemeiner, P.; Tkac, J. *Microchimica Acta* **2013**, *180*, 151(b) Bertok, T.; Sediva, A.; Katrlik, J.; Gemeiner, P.; Mikula, M.; Nosko, M.; Tkac, J. *Talanta* **2013**, *108*, 11.

(27) (a) Kim, D.; Chae, M. K.; Joo, H. J.; Jeong, I.-h.; Cho, J.-H.; Lee, C. *Langmuir* **2012**, *28*, 9634(b) Kim, G.; Yoo, C. E.; Kim, M.; Kang, H. J.; Park, D.; Lee, M.; Huh, N. *Bioconjugate Chemistry* **2012**, *23*, 2114(c) Chen, S.; Liu, L.; Jiang, S. *Langmuir* **2006**, *22*, 2418(d) Ostuni, E.; Chapman, R. G.; Liang, M. N.; Meluleni, G.; Pier, G.; Ingber, D. E.; Whitesides, G. M. *Langmuir* **2001**, *17*, 6336.

(28) Tkac, J.; Davis, J. J. *Journal of Electroanalytical Chemistry* **2008**, *621*, 117.

(29) Davis, J. J.; Tkac, J.; Laurenson, S.; Ferrigno, P. K. *Analytical chemistry* **2007**, *79*, 1089.

(30) (a) Volkert, A. A.; Subramaniam, V.; Ivanov, M. R.; Goodman, A. M.; Haes, A. J. *ACS Nano* **2011**, *5*, 4570(b) Dong, Y.; Abaci, S.; Shannon, C.; Bozack, M. J. *Langmuir* **2003**, *19*, 8922.

(31) Lahiri, J.; Isaacs, L.; Tien, J.; Whitesides, G. M. *Analytical Chemistry* **1999**, *71*, 777.

(32) Cairo, C. W.; Gestwicki, J. E.; Kanai, M.; Kiessling, L. L. *Journal of the American Chemical Society* **2002**, *124*, 1615.

(33) Davis, J. J.; Tkac, J.; Humphreys, R.; Buxton, A. T.; Lee, T. A.; Ko Ferrigno, P. *Analytical chemistry* **2009**, *81*, 3314.

(34) Becker, J. W.; Reeke, G. N.; Wang, J. L.; Cunningham, B. A.; Edelman, G. M. *Journal of Biological Chemistry* **1975**, *250*, 1513.

(35) Bouckaert, J.; Poortmans, F.; Wyns, L.; Loris, R. *Journal of Biological Chemistry* **1996**, *271*, 16144.

(36) (a) Yu, L.; Huang, M.; Wang, P. G.; Zeng, X. *Analytical Chemistry* **2007**, *79*, 8979(b) Zhang, Y.; Luo, S.; Tang, Y.; Yu, L.; Hou, K.-Y.; Cheng, J.-P.; Zeng, X.; Wang, P. G. *Analytical Chemistry* **2006**, *78*, 2001.